16

Fabrication of Double-Stranded DNA Microarray on Solid Surface for Studying DNA-Protein Interactions

A High-Throughput Platform for Profiling Bimolecular Interaction

JINKE WANG AND ZUHONG LU
Chien-Shiung Wu Laboratory, Southeast University, Nanjing 210096, China

Abstract: This paper presents two novel methods for fabricating double-stranded DNA (dsDNA) microarray. In the first method, the presynthesized single-stranded DNA (ssDNA) oligonucleotides containing two reverse complementary sequences at their 3′ hydroxyl end were firstly immobilize on the surface of the aldehyde-derivatized glass slides by their 5′ end, and then the two reverse complementary sequences were annealed to form a short dsDNA hairpin structure which provided the primer for later polymerase elongation. Finally, the ssDNA microarrays were converted into the unimolecular dsDNA microarrays by an on-chip polymerase reaction. In the second method, the two kinds of ssDNA oligonucleotides named constant oligonucleotide (CO) and target oligonucleotides (TOs) were synthesized. Then the different TOs harboring the DNA-binding sites were respectively annealed and ligated with the same CO containing an internal aminated dT in tubes. The reaction products were immobilized on the surface of the aldehyde-derivatized glass slides by the aminated dT to fabricate the partial-dsDNA microarrays. Finally, the partial-dsDNA microarrays were converted into the unimolecular dsDNA microarrays by an on-chip polymerase reaction. The excellent efficiency and high accuracy of the enzymatic synthesis in two methods were demonstrated by incorporation of fluorescently labeled dUTPs in Klenow extension and the digestion of dsDNA microarrays with restriction endonuclease. The accessibility and specificity of the DNA-binding proteins binding to dsDNA microarrays were verified by binding Cy3 labeled NF-κB (p50) to dsDNA microarrays. Therefore, the dsDNA microarray containing 66 probes representing 30 all-possible single-nucleotide mutant NF-κB binding targets of Ig-κB and 36 wild-type NF-κB binding targets were fabricated to determine the binding affinities of NF-kB homodimer p50 to all probes on chip. We found the binding results were very consistent with that from x-ray crystallography

studies and gel mobility-shift analysis. The unimolecular dsDNA microarray has great potentials to provide a high-throughput platform for investigating the sequence-specific DNA-protein interactions involved in gene expression regulation, restriction and so on.

Key words: Double-stranded DNA microarray, fabrication, DNA-protein interactions.

1. Introduction

The interactions of DNA-binding proteins and DNA-binding drugs with double-stranded DNA (dsDNA) in genome are involved in many important biological functions, including gene transcription regulation (1), DNA recombination (2), restriction (3), replication (4) and DNA-drugs intercalation (5,6). Therefore, lots of techniques were used to effectively study DNA-drugs interaction,including nitrocellulose-binding assays (7), gel mobility-shift analysis (8,9), Southwestern blotting (10,11), ELISA (12), reporter constructs in yeast (13), Chromatin immunoprecipitation (ChIP) (14), phage display (15), binding-site signatures (16), in-vitro selection (17), UV crosslinking (18), and methylization interfering assay (19), X-ray crystallography (20,21) were developed to effectively examine sequence-specific DNA-protein interactions, and also techniques including UV absorption(22), melting temperature (thermodynamics) (23), NMR (24), X-ray crystallography (25), free solution capillary electrophoresis (FSCE) (26), scanning force microscopy (SFM) (27,28,29), atomic force microscopy (AFM) (30), surface plasmon resonance (SPR) (31), polymerase chain reaction (PCR) (32) and footprinting (33). However, these techniques using solvent dsDNAs to probe dsDNA interactions with other molecules as proteins, ligands and drugs suffered from being laborious, time-consuming and incapable of high-parallel analysis. Therefore, the solid surface-coupled dsDNA had become more and more important for high-throughput examination of sequence-specific DNA/protein (34) and DNA/drug interactions (35,36), it paved the way to new strategies for screening DNA-binding proteins(37), predicting DNA binding sites (38,39), assessing binding affinity (35,36), and screening sequence-specific DNA-binding drugs and finding drugs preferential sequences (35,36).

As the surface-coupled homogenous dsDNAs are employed to examination of the sequence-specific DNA/proteins or DNA/drugs interactions, the number of classes of dsDNAs immobilized on a detectable solid entity determines how much information could be obtained in a single study. The cellulose or agarose-coupled homogenous dsDNAs were traditionally used to isolate the sequence-specific DNA-binding proteins (40,41) by the affinity chromatography, and the small paramagnetic particles-attached homogenous dsDNA probes were used to identify DNA-binding proteins by matrix-assisted laser

desorption/ionization time-of-flight mass spectrometry (MALDI-TOF MS) (37). However, these solid entities carrying homogenous dsDNAs suffered from isolating or identifying only one target molecular every time. Therefore, they were not the high informative strategies for surface-coupled dsDNA applications. Comparatively, the libraries of dsDNA oligonucleotides comprising a plurality of different members immobilized on solid support much improved the limitation (42). These solid-immobilized libraries of dsDNA oligonucleotides provided a useful technique for the screening of numerous biological samples by sequence-specific interactions (42). Thereafter, the fabrication of fast, economical and high informative dsDNA-coupled solid entities became the pivotal problem for extensive surface-coupled dsDNA applications. Nevertheless, the earliest surface-immobilized libraries of different dsDNA oligonucleotides were fabricated by immobilizing very long chemically-synthesized single-stranded DNA (ssDNA) oligonucleotides on solid surface and then forming unimolecular dsDNA oligonucleotides by intrastrand annealing self-complementery elements in immobilized long single-stranded oligonucleotides (42). This kind of surface-coupled dsDNA were high informative, but suffered from economic issues.

The appearance of high density bimolecular dsDNA microarray greatly promoted the application of solid-immobilized duplex nuclei acids (34, 35, 36, 38, 39). It was demonstrated that these high density bimolecular dsDNA microarrays were very effective for high throughput examination of DNA-proteins interaction (38, 39). However, the developments of these bimolecular dsDNA microarrays were impeded by several innate technical and economic drawbacks. The current-developed methods manufacturing bimolecular dsDNA microarrays could be divided into two types, one was by hybridization (35, 36, 43) and the other was enzymatic elongation (34). The former spotted larger number of chemically synthesized ssDNA oligonucleotides onto solid surface to firstly fabricate ssDNA microarray and subsequently converted ssDNA microarray into bimolecular dsDNA microarray by hybridizing the ssDNA microarray with a mixture of complementary ssDNA oligonucleotides. This method suffered from two main problems, one was high costs of the synthesis of the complementary ssDNA oligonucleotides and amino-modification of immobilized ssDNA oligonucleotides, the other more important problem was that the method could not fabricate dsDNA microarrays carrying very sequence-similar probes such as probes with single-nucleotides variation (35, 36). The latter on-chip photo-addressably synthesized high density ssDNA microarray with a constant sequence at far surface-attached 3′ end of each oligonucleotides, and then annealed a general primer to constant sequence and performed enzymatic extension reaction on array to convert ssDNA microarray into bimolecular dsDNA microarray. This method encountered more serious economic and technical issues. In technique, the method replied on currently expensive and proprietary technology of surface photo addressable synthesis of oligonucleotides, but the synthesis of single-stranded oligonucleotides on

solid surface was inefficient, with per-nucleotide synthesis efficiencies thought to be only 92-96% (44, 45). For 40-mer oligonucleotides, only 4-20% of the sequences on a chip could be of desired length and sequence (46). In practice, oligonucleotide arrays constructed in this fashion were heavily contaminated with truncated molecules (44, 47). Moreover, the presence of so many competing truncated molecules and single-stranded oligos not accessible to the primers might strongly interfere and mislead binding experiments (46). Finally, considering the possible instability of bimolecular dsDNA oligos in binding or washing reactions, the utility efficiency of this kind of bimolecular dsDNA microarrays might be lowered.

The alternative route to construct dsDNA arrays might resolve the economic and technical problems. Ben-Yoseph and his co-workers fabricated the dsDNA microarray by hybridization and ligation. These investigators attached single-stranded oligonucleotides to gold supports by a thiol linkage, and then to those oligos, hybridized and ligated double-stranded DNAs with the appropriate complementary ends (43). Bulyk and his co-workers fabricated the dsDNA microarray by hybridization and polymerization (38). The alternative methods for dsDNA microarray fabrication promoted the practical application of dsDNA microarray. For example, the dsDNA microarrays, fabricated by microspotting the dsDNA oligonucleotides which were prepared by firstly annealing the set of 64 oligonucleotides representing all possible 3-nt central-finger sites for Zif268 zinc finger with a 5′ amino-tagged universal primer and subsequently polymerizing with Klenow enzyme, were effectively used to explore the DNA-binding specificities of zinc fingers (38). Nevertheless, the utility efficiency of the bimolecular dsDNA micorarray must be lowered by the possible denature of bimolecular dsDNA probes in remove of the bound proteins for more hybridizations.

To overcome the drawbacks existing in the above described dsDNA microarray techniques, we presented two new methods for fabricating unimolecular dsDNA microarray which can be used for many times. First was to immobilize ssDNA oligonucleotides by 5′ end which contained two reverse complementary sequences at 3′ hydroxyl end, and then annealed two reverse complementary sequences to form a short dsDNA hairpin structure which took the role of primer for later polymerization. After an on-chip polymerase elongation reaction, the single-stranded microarrays were converted into unimolecular dsDNA microarrays. Second was to synthesize two kinds of ssDNA oligonucleotides called constant oligonucleotide and target oligonucleotide. The constant oligonucleotide with internal aminated dT was used to capture and immobilize the target oligonucleotides onto solid surface, and also provide primer for later enzymatic extension reaction, while target oligonucleotides took the role of houbouring DNA-binding sites of DNA-binding proteins. The variant target oligonucleotides were annealed and ligated with the constant oligonucleotide to form the new unimolecular oligonucleotides for microspotting. The prepared unimolecular oligonucleotides were microspotted on aldehyde-derivatized glass slides to make

partial-dsDNA microarray. At last, the partial-dsDNA microarray was converted into unimolecular complete-dsDNA microarray by a DNA polymerase extension reaction. The excellent efficiency and high accuracy of the enzymatic synthesis in two methods were demonstrated by incorporation of fluorescently labeled dUTPs in Klenow extension and digestion of dsDNA microarrays with restriction endonuclease. The accessibility and specificity of the DNA-binding proteins binding to dsDNA microarrays were verified by binding Cy3 labeled NF-κB to dsDNA microarrays. We fabricated the dsDNA microarray containing 31 probes representing the wild-type and all-possible single-nucleotide mutant NF-κB binding targets of Ig-κB, to determined the binding affinities of NF-kB homodimer p50 to all probes on chip. We found the binding results were very consistent with that from x-ray crystallography studies and gel mobility-shift analysis. The dsDNA microarrays we fabricated have great potentials to provide a high-throughput platform for investigation of sequence-specific DNA-protein interactions involved in gene expression regulation, restriction and so on.

2. Materials and Methods

2.1 Manufacture of Double-Stranded DNA Microarray

The special ssDNA oligonucleotides listed in tables were chemically synthesized by Shengyou Inc. (Shanghai, China) for manufacturing dsDNA microarrays.

In method 1, the ssDNA oligonucleotides were designed and chemically synthesized as materials to fabricate ssDNA microarray. The prepared single-stranded oligonucleotides contained the seven elements consisting of 5′ NH_2—proximal flanking sequence—restriction endonuclease digestion site—DNA-binding protein binding consensus—distal flanking sequence—reverse complementary sequence—hairpin loop bases—reverse complementary sequence 2—3′ OH as listed in Table 16.1. We also synthesized single-stranded oligonucleotides which elements including proximal flanking sequence, restriction endonuclease digestion site and hairpin loop bases were varied as listed in table 16.1 too. The dsDNA microarrays were fabricated according to the scheme displayed in Figure 16.1. Firstly, the 5′-end amino-linked oligonucleotides were printed on glutaraldehyde-derived glass slides to fabricate the single-stranded oligonucleotides microarray. Secondly, the slides were incubated with boiling water to denature the possible partial hairpin structure. Thirdly, the slides were incubated with hybridization buffer to form the hairpin structure primer at the free end of immobilized oligonucleotides. Fourthly, the slides were incubated with Klenow enzyme reaction solution to extent the hairpin primer.

In method 2, the two kinds of ssDNA oligonucleotides named the constant oligonucleotide (CO) and the target oligonucleotides were designed and

TABLE 16.1. Single-stranded oligonucleotides prepared by chemical synthesis

		Sequence (5′→ 3′)				
Group	No.	FS (or SP)	PBS	RS	LB	RS
1	SS	AGTTGAG	GGGACTTTCC	CAGGC	TT	
2	FS0	GAATTC	GGGACTTTCC	CAGGC	TT	GCCTG
	FS1	TGAATTC	GGGACTTTCC	CAGGC	TT	GCCTG
	FS2	TTGAATTC	GGGACTTTCC	CAGGC	TT	GCCTG
	FS3	TTTGAATTC	GGGACTTTCC	CAGGC	TT	GCCTG
	FS4	TTTTGAATTC	GGGACTTTCC	CAGGC	TT	GCCTG
	FS5	TTTTTGAATTC	GGGACTTTCC	CAGGC	TT	GCCTG
3	RS2	TTTTGAATTC	GGGACTTTCC	CA	TT	TG
	RS3	TTTTGAATTC	GGGACTTTCC	CAG	TT	CTG
	RS4	TTTTGAATTC	GGGACTTTCC	CAGG	TT	CCTG
4	LB0	TTTTGAATTC	GGGACTTTCC	CAGGC		GCCTG
	LB1	TTTTGAATTC	GGGACTTTCC	CAGGC	T	GCCTG
	LB2	TTTTGAATTC	GGGACTTTCC	CAGGC	TT	GCCTG
	LB3	TTTTGAATTC	GGGACTTTCC	CAGGC	TTT	GCCTG
5	A3	AAAGGTTCCTT	GGGTTCCTTT	CAGGC	TT	GCCTG
	Lac-rep	AATTGTGAGCGG	AT AACA ATT	CAGGC	GCCTG GCCTG	GCCTG
	CAP	TGTG AGT	TAGCTCACT	CAGGC	GCCTG GCCTG	GCCTG
	GAL4	CGG AGGAC	AGTCCTCCG	CAGGC	GCCTG GCCTG	GCCTG
	TFIID	CTGTGCA	TATAA	CAGGC		GCCTG
	GCN4	AGCGGA	ATGACTCAT	CAGGC	GCCTG GCCTG	
	AP1	CGCTTGA	TGAGTCA	CAGGC	GCCTG GCCTG	
	AP2	AATGTCC	CCGCGGC	CAGGC	GCCTG GCCTG	
	SP1	ACGATCG	GGGCGG	CAGGC		GCCTG

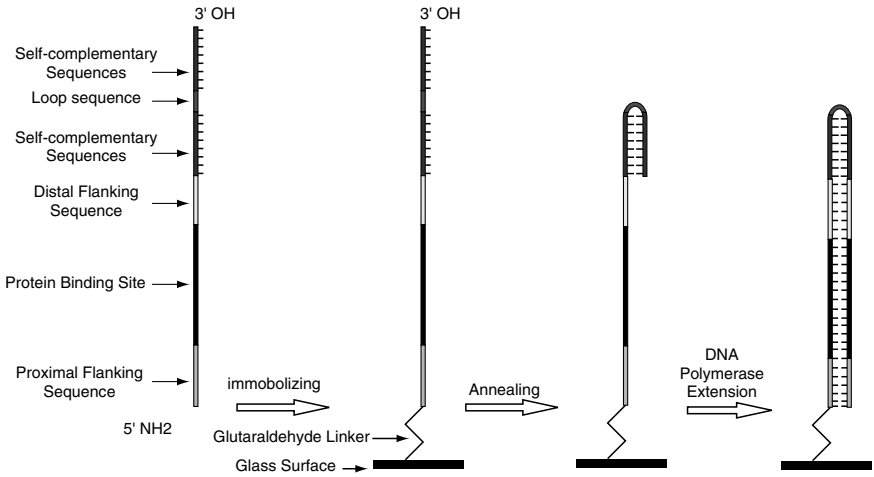

FIGURE 16.1. The scheme for dsDNA microarray fabrication with method 1 and verification with enzymatic digestion.

chemically synthesized as materials to fabricate ssDNA microarray. The CO contained a 7-base single-stranded capture overhang at 3′ end and two reverse self-complementary sequences intervened by an internal dT with a primary NH_2 group (amino modifier C6) at 5′ end. The TOs consisted of the 7-base general proximal flanking sequence complementary to capture overhang on CO, target sequence containing 10-base wild or single-nucleotide mutated Ig-κB sites, and the 7-base general distal flanking sequence from 3′ to 5′ end. The CO contained hydroxyl at 3′ end and phosphate at 5′ end, and the TOs had hydroxyl at both 3′ and 5′ ends. The dsDNA microarrays were fabricated according to the scheme displayed in figure 16.7. The different TOs were respectively annealed and ligated with the same pre-self-annealed COs in 1:1 molar ratio in a ligation reaction containing 40 mM Tris-HCl (pH 7.8), 10 mM $MgCl_4$, 10 mM DTT, 0.5 mM ATP and 0.5 U/μl T4 DNA ligase (MBI fermentas). The completed ligation reactions were exchanged into sodium carbonate buffer (0.1M, pH9.0) at a concentration of 50 μM for microspotting, by using CentriSpin-10 spin columns (Princeton Separations, Adelphia, NJ).

The cleaned microscopy glass slides were silanized in 2% aminopropyltriethoxysilane (Sigma) dissolved in 95% acetone for 5 min. After rinsing twice with acetone and then baked for 45 min at 75 ˚C, the silanized slides were activated in glutaraldehyde solution (5% glutaraldehyde, 0.01M PB, pH7.0) for 30 min. The slides were then washed thoroughly with distilled water and blow to dry with N_2. The glutaraldehyde-treated glass slides were stored at 4 ˚C and used in 15 days. A pin-based spotting robot PixSys5500 (Cartesian Technology Inc.) with a CMP3 pin was employed to print the prepared

oligonucleotides dissolved in sodium carbonate buffer (0.1M, pH9.0) on slides. After printing, the microarrays were incubated overnight at room temperature, then for 1 h at 37 ˚C in a humidity chamber containing sodium carbonate buffer (0.1M, pH9.0). The rest of the aldehyde surface was inactivated by a 30-min incubation in 0.28% (w/v) $NaBH_4$/76% (v/v) PBS/24% (v/v) alcohol. After sufficiently washing in sterile ddH_2O, the microarrays were spun dry in a clinical centrifuge.

The dried microarrays were incubated in boiling sterile water for 5min and then treated with hybridization buffer for 1 h at 50 ˚C. The annealed microarrays were respectively washed with 2×SSC/0.1% SDS and 0.2×SSC/0.1% SDS for 10min at room temperature. After washing sterile ddH_2O and dry in a clinical centrifuge, the microarrays were incubated with DNA polymerase reaction containing 50 mM Tris-HCl (pH 7.2), 10 mM $MgSO_4$, 0.1 mM DTT, 40 μM of each dNTP, 20μg/ml acetylated BSA and 2 U/μl DNA polymerase I large (Klenow) fragment (3′ to 5′ exo^-; Promega, Madison, WI). After extension reaction, the microarrays were respectively washed with 2×SSC/0.1% SDS, 0.2×SSC/0.1% SDS and sterile ddH_2O for 10min at room temperature. At last, the microarrays were dried in a clinical centrifuge and kept in closed cassette at 4 ˚C until use.

2.2 NF-κB (p50-p50) Binding to dsDNA Microarray

Transcription factor NF-κB, human recombinant p50 expressed in bacteria from a full-length cDNA encoding 453 amino acids, was purchased from Promega (Madison, WI). The protein provided in glycerol solutions were transferred to sodium carbonate-sodium bicarbonate buffer (pH9.3) and labeled with FluoroLinkTM Cy3 monofunctional dye (Amersham Pharmacia Biotech, Piscataway, NJ) at room temperature for 30min. After labeling, the protein were exchanged into glycerol-free, phosphate-buffer saline (PBS) solution (141 mM NaCl, 7.2 mM Na2HPO4, 2.8 mM NaH2PO4, pH7.4) by BioRad Biospin P6 column. The labeled proteins PBS solutions were kept at 4 ˚C until use. The dsDNA microarrays were blocked with 10% BSA for 1 h at room temperature, then incubated with DNA-binding buffer (10mM HEPES pH7.9, 50mM KCl, 2.5mM DTT, 0.1mM EDTA, 0.05% NP-40, 10% Glycerol, 5%BSA) containing Cy3 labeled NF-κB (p50) at room temperature for 1 h. After incubation, the microarrays were in turn washed with PBS/0.05% Tween 20 for 15 min, PBS/0.01% Triton 100 for 15 min, and PBS for 15 min at room temperature. After spinning dry in a clinical centrifuge, the microarrays were scanned with ScanArray® Lite of Packard Biochip Technologies in the Cy3 channel at 90% laser power, 80% PMT gain, 5 μm resolution.

2.3 dsDNA Microarray Data Analysis

The signal intensities of the spots on microarray scanned false color images were quantified QuantArray® microarray analysis software (Packard

Biochip Technologies). The signal intensities of the spots referred to the absolute signal intensities arrived from substracting the background fluorescence intensities from detected signal intensities of spots. The relative signal intensities of spots of the single-nucleotide mutated I*g*-κB targets were calculated as a fraction of the averaged intensity of spots of the wild-type I*g*-κB targets.

3. Results

3.1 Manufacture of dsDNA Microarray

3.1.1 Manufacture of dsDNA Microarray with Method 1

3.1.1.1 Design of Oligonucleotides for Fabricating the ssDNA Microarray

The prepared ssDNA oligonucleotides were characterized with containing two reverse self-complementary sequences at their 3′ end and an overhang sequence at 5′ end. The two reverse self-complementary sequences linked by loop bases were constituted by the same number of bases, and were used to form a short dsDNA hairpin structure which played the role of primer for enzymatic extension. The overhang sequence contained the DNA-binding site of transcription factors NF-kB and flanking sequence (or spacing sequence) from 3′ end to 5′ end. The overhang sequence was used as template for enzymatic extension. The DNA-binding site of transcription factors NF-kB was used to explore the accessibility of synthesized unimolecular dsDNA oligonucleotide immobilized on chip to DNA-binding protein, NF-kB. The flanking sequence at the far 5′ end served as the arm molecules to avoid the possible steric hindrance from solid surface to DNA/protein interaction. In some oligonucleotides, a HaeIII digestion sites were harbored in flanking sequence to verify the enzymatic synthesis and the accessibility of sequence-specific restriction endonuclease to its target site harbored in immobilized dsDNA. The 5′ end of all synthesized oligonucleotides were modified with one primary amino group, which was used to immobilize the oligonucleotides on aldehyde-derived glass slide surface. The 3′ end of all synthesized oligonucleotides were hydroxyl group, which was used to primer extension. Oligonucleotides with various flanking sequences, reverse complementary sequences and loop bases were synthesized to investigate their influences on enzymatic synthesis, it aims at optimizing the oligonucleotides design for fabricating the most economical and effective dsDNA microarrays with the method provided.

3.1.1.2 Scheme of dsDNA Microarray Fabrication

The scheme of dsDNA microarray fabrication used in this paper is illustrated in Figure 16.1. According to the scheme, dsDNA microarray will be fabricated with three steps. Firstly, the amino-linked oligonucleotides were printed

on aldehyde-derived glass slides to fabricate the ssDNA oligonucleotides microarrays. Secondly, the ssDNA oligonucleotides microarrays were denatured with boiling sterile distilled water and then reannealed in hybridization buffer to form partial-ssDNA oligonucleotides microarrays with hairpin primer at the free 3′ end of immobilized oligonucleotides. Thirdly, the partial-ssDNA oligonucleotides microarrays were incubated with Klenow extension reaction to form complete-dsDNA oligonucleotides microarrays.

3.1.1.3 Verification of the Enzymatic Extension of Hairpin Primer

The most important thing for our dsDNA microarray fabrication method is to corroborate DNA polymerase successfully performed nucleotide polymerization from the special hairpin primer on the short template immobilized on solid surface. In order to verify the enzymatic extension of hairpin primer, three ssDNA microarrays were fabricated by spotting oligonucleotide No.A3 in Table 16.1 on glass slides in 4×4 format (A3 ssDNA microarray). One A3 ssDNA microarray was incubated with a Klenow extension reaction including Cy3-labled dUTP, unlabeled dGTP, dCTP and dATP, and other two A3 ssDNA microarrays were respectively treated with a reaction containing Klenow plus four unlabeled dNTPs and a reaction including Cy3-labled dUTP, unlabeled dGTP, dCTP and dATP but no Klenow as control fabrications. At the same time, we also fabricated the ssDNA microarray by spotting oligonucleotide No.SS in Table 16.1 on glass slides in 4×4 format (SS ssDNA microarray), and incubated it with a Klenow extension reaction including Cy3-labled dUTP, unlabeled dGTP, dCTP and dATP also as control fabrication. As expected, the fluorescent signals of spots were seen over the entire arrays incubated with Klenow extension reaction containing Cy3-dUTP, dGTP, dCTP and dATP (Figure 16.2A). However, no signal intensity

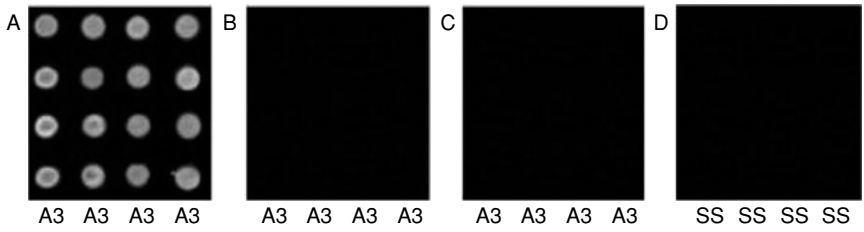

FIGURE 16.2. Fluorescence images of dsDNA microarrays. Image of (A) is dsDNA microarray fabricated with a Klenow extension reaction including Cy3-labled dUTP, unlabeled dGTP, dCTP and dATP. Image of (B) is dsDNA microarray fabricated with a Klenow extension reaction including four unlabeled dNTPs. Image of (C) is dsDNA microarray fabricated with a reaction including Cy3-labled dUTP, unlabeled dGTP, dCTP and dATP but no Klenow enzyme. Image of (D) is ssDNA microarray incubated with a reaction including Klenow, Cy3-labled dUTP, and unlabeled dGTP, dCTP and dATP.

appeared over the three control ssDNA microarrays (Figure 16.2B, 2C and 2D).

As the oligonucleotide No.A3 was designed only containing three adenines at the far 5′ end, therefore, the fluorescent signals of spots appearing on dsDNA microarray of Figure 16.2A demonstrated that not only the hairpin primer has successfully formed, but also the DNA polymerase Klenow fragment enzyme successfully performed nucleotides polymerization reactions to the far 5′ end of immobilized single-stranded oligonucleotides. No signal intensities appearing over the three control ssDNA microarrays verify that the fluorescent signals on dsDNA microarray of Figure 16.2A really depend on the reaction of DNA polymerase Klenow fragment incorporating Cy3-labled dUTP in hairpin primer extension. The results demonstrate that it is feasible to manufacture dsDNA microarrays with the method hairpin primer extension.

The homogeneity of the dsDNA polymerization reactions on larger microarray was also demonstrated by the following 10×30 microarray fabrication (Figure 16.3).

3.1.1.4 Accessibility of Enzymatically Synthesized dsDNA Microarray to DNA-Binding Protein

Because the electrostatic properties at the solid–liquid interface and the local ionic strength of the immobilized dsDNA molecules are greatly different from that in the bulk solution, the interfacial effect can influence the molecular interactions at the solid–liquid interface, especially when the functional motif of molecule becomes increasingly closer to solid surface. Because the dsDNA synthesized on glass slides in our above preliminary experiments was very short (26 bases), as soon as the feasibility of dsDNA microarrays manufacture with hairpin primer extension was confirmed, we expected to find whether the short dsDNA fabricated on array slides was accessible to target

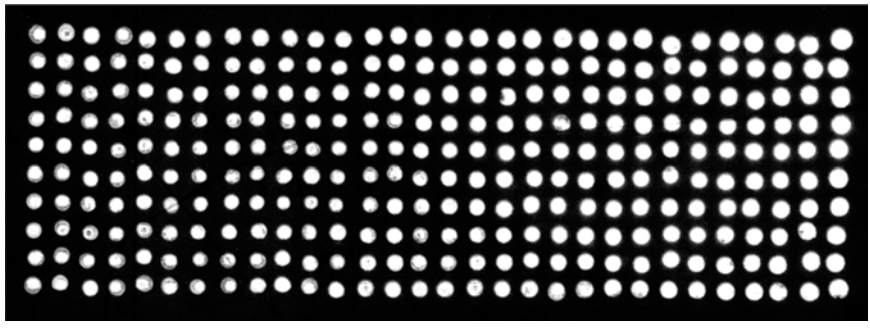

FIGURE 16.3. Large homogeneous dsDNA microarray fabricated with Cy3-labeled dUTP incorporation in polymerization reactions.

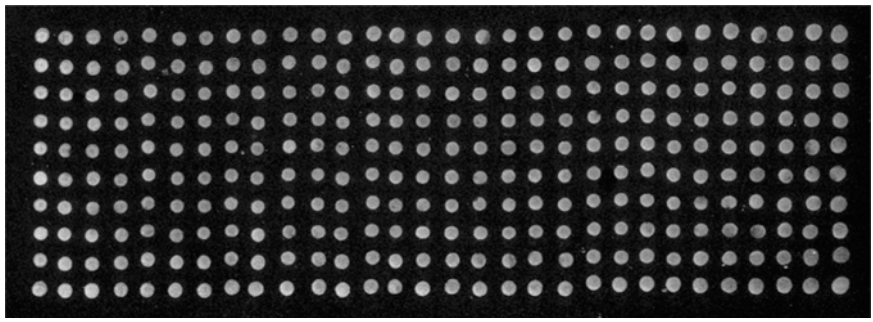

FIGURE 16.4. Large homogeneous dsDNA microarray fabricated with Cy3-labeled dUTP incorporation and dsDNA microarray fabricated with dNTP incorporation which bound by Cy3-labeled NF-kB homodimer p50.

sequence-specific DNA-binding proteins in sample before we do any more successive experiments. Therefore, we synthesized an oligonucleotide which contained a 10-base NF-kB binding site (No. FS5 in Table 16.1) and fabricated a 10×30 dsDNA array by enzymatically incorporating unlabeled dNTP. The fabricated dsDNA microarray was hybridized with Cy3 labeled NF-kB.

The hybridization results revealed that the short dsDNA enzymatically synthesized on glass surface can significantly be bound by Cy3 labeled NF-kB in sample as showed in Figure 16.4. The signal intensities between different spots were very homogeneous. Because only 11 irrelevant base pairs flank the NF-kB binding site in the immobilized dsDNA oligonucleotides, it demonstrates that short spacing distance between glass surface and NF-kB binding site did not prevent the interaction of dsDNA-binding site on glass surface with NF-kB in sample. It also suggested that the spacing distance of 11-base pairs may not be the threshold distance which prevents DNA/protein interaction.

3.1.1.5 Optimizing the ssDNA Oligonucleotides Design

As the feasibility of manufacturing dsDNA microarrays with the method of hairpin primer extension and accessibility of DNA-binding proteins to dsDNA microarrays had confirmed, we wanted to know how long flanking sequence, reverse complementary sequence and loop bases were most economical but effective for dsDNA microarrays fabrication with hairpin primer extension. Therefore, we designed and synthesized three groups of amino-linked single-stranded DNA oligonucleotides displayed in Group 3, 4 and 5 in Table 16.1, which had various flanking sequence, reverse complementary sequence and loop bases in different lengths. We fabricated the ssDNA microarrays by spotting these oligonucleotides on slides in quadruplet format. The fabricated ssDNA microarrays were annealed and then extended

with Klenow reaction including Cy3-labeled dUTP, and unlabeled dGTP, dCTP and dATP.

Figure 16.5A displays the fluorescence image of dsDNA microarray fabrication with Cy3-labeled dUTP incorporation. It is clear that the fluorescence intensities of different oligonucleotides are not the same (Figure 16.4B). This demonstrates that the variability of the length of flanking sequence, hairpin loop sequence and reverse complementary sequence can influence the efficiency of Cy3-labeled dUTP incorporation, that is, the efficiency of enzymatic extension reaction. The characteristics of fluorescence intensities of various oligonucleotides revealed that the dsDNA microarray manufacture with enzymatic extension of hairpin primer followed several general laws. First, the efficiency of enzymatic extension reaction enhanced with the increasing length of flanking sequence. The longer of flanking sequence, the easier of enzymatic extension reaction. This may result from the steric hindrance of glass surface to enzymatic extension reaction on surface-near DNA template. Second, the efficiency of enzymatic extension reaction dramatically decreased with the shortening of reverse complementary sequence. It was clear that the longer reverse complementary sequences benefited enzymatic extension reaction, because the longer reverse complementary sequences could more easily form more stable double-stranded hairpin structure which provides the primer for enzymatic extension reaction. Third, the efficiency of

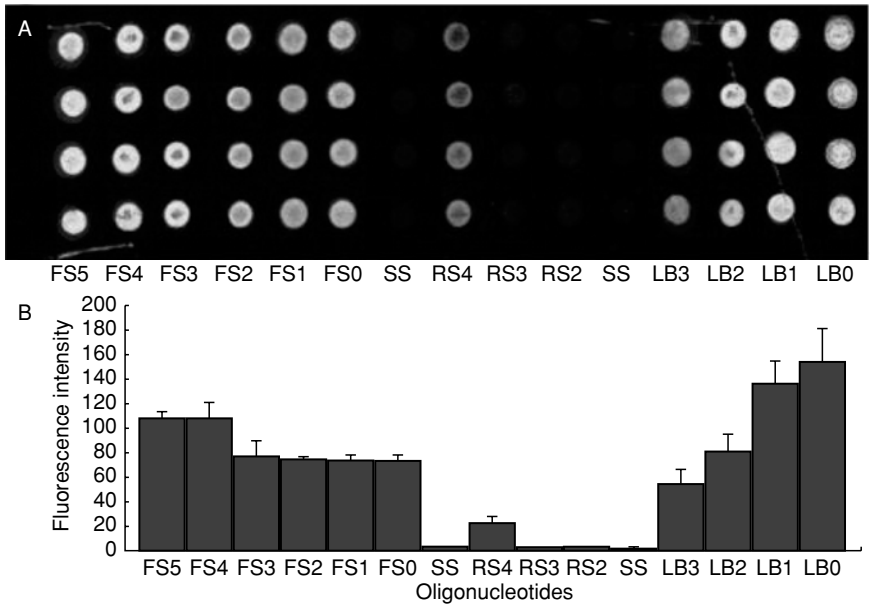

FIGURE 16.5. dsDNA microarray fabricated with Cy3-labeled dUTP incorporation and dsDNA microarray fabricated with dNTP incorporation. The image verified the efficiencies of different single-stranded oligonucleotides for dsDNA microarray fabrication.

enzymatic extension reaction increased with the decrease of loop bases. No loop base resulted in the most effective enzymatic extension reaction. It seems that few loop bases were more beneficial for hairpin structure formation. Therefore, we concluded that the longer flanking sequence, no loop base and the longer reverse complementary sequence are most effective for dsDNA microarray fabrication with hairpin primer extension.

Successively, we confirmed the above characters of dsDNA microarray fabrication with enzymatic extension reaction by binding DNA-binding protein with dsDNA microarray. We fabricated the dsDNA microarrays with same oligonucleotides by Klenow incorporation of unlabeled dNTPs, and hybridized the fabricated dsDNA microarray with Cy3-labeled transcription factor NF-kB. The results showed that all dsDNA oligonucleotides fabricated on microarray were accessible to NF-kB. However, the efficiency of NF-kB binding to various dsDNA probes on microarray was different (Figure 16.5A), and the variation of fluorescence intensities of different dsDNA probes bound by NF-kB (Figure 16.5B) was coincident with that of dsDNA microarray fabrication by enzymatic incorporation of Cy3-labeled dUTP (Figure 16.4A). It suggested that the more dsDNA probes fabricated on spots, the more DNA-binding proteins bound on them. Therefore, we adopted to synthesize the single-stranded oligonucleotides with no loop base and longer reverse complementary sequence (5 bases) to do the latter experiments.

3.1.1.6 Specificity of Interaction of dsDNA Microarray with DNA-Binding Proteins

The sequence-specificity of interactions of dsDNA consensus harbored in immobilized short dsDNA oligonucleotides with their target DNA-binding proteins as transcription factors is critical the most important thing for the applications of dsDNA microarray, because the dsDNA microarray we fabricated mainly focused on screening sequence-specific DNA-binding proteins. To verify the specificity, we synthesized 8 different amino-linked oligonucleotides which respectively contained one DNA-binding site corresponding to one of 8 typical transcription factors from bacteria to human being as listed in Group 8 of Table 16.1. The dsDNA microarray was fabricated with the 8 oligonucleotides and oligonucleotide No. LB0 in Table 16.1 which contains the DNA-binding sites of NF-kB. We hybridized the fabricated dsDNA microarray with Cy3 labeled transcription factors NF-kB.

Figure 16.6 showed the results of the dsDNA microarray hybridized with Cy3-labeled transcription factors NF-kB. It demonstrates that all dsDNA-binding sites of NF-kB were specifically identified and bound by Cy3 labeled transcription factors NF-kB in sample. However, dsDNAs containing other transcription factors were not bound by NF-kB, except little non-specific absorption which could be eliminated by more stringent washing. This primary experiment with DNA-binding proteins NF-kB implies that dsDNA microarray fabricated by hairpin primer extension has great potential to

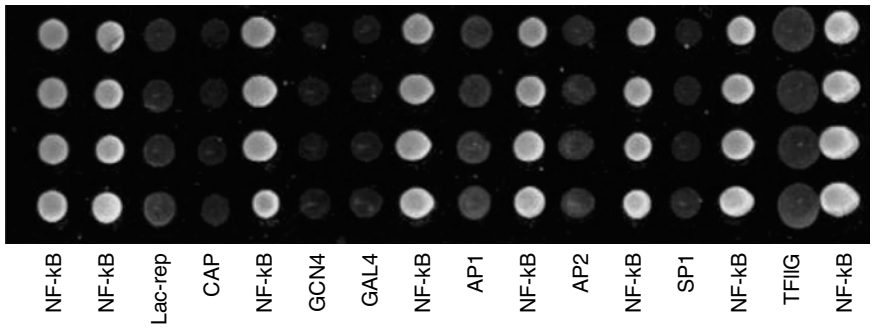

FIGURE 16.6. dsDNA microarray containing 9 different DNA-binding proteins targets which bound by Cy3-labeled NF-kB homodimer p50. The image demonstrated the sequence-specificity of interaction between arrayed dsDNA with protein.

provide a high-throughput technique for DNA-binding proteins screening and DNA/protein interactions.

3.1.2 Manufacture of dsDNA Microarray with Method 2

3.1.2.1 Design of Oligonucleotides for Fabricating the ssDNA Microarray

Two kinds of ssDNA oligonucleotides, constant oligonucleotide (CO) and the target oligonucleotides (TOs), were chemically synthesized to fabricate ssDNA microarray in method 2 (Table 16.2). The CO contained a 7-base single-stranded capture overhang at 3′ end and two reverse self-complementary sequences intervened by an internal dT with a primary NH_2 group (amino modifier C6) at 5′ end. The TOs consisted of the 7-base general proximal flanking sequence complementary to capture overhang on CO, target sequence containing 10-base wild-type or single-nucleotide mutant Ig-κB sites, and the 7-base general distal flanking sequence from 3′ to 5′ end. The

TABLE 16.2. Oligonucleotides synthesized to fabricate dsDNA microarray

		Sequences (5′ →3′)		
	##.	Distal Flanking sequence	Target sequence	Proximal Flanking sequence
Target Oligonucleotide	AP1	CGCTTGA	TGAGTCA	CGTACGC
	AP2	AATGTCC	GCCCGCGGC	CGTACGC
	SP1	ACGATCG	GGGCGG	CGTACGC
	TFIID	CTGTGCA	TATAA	CGTACGC
	NF-kB (NS)	AGTTGAG	GGGACTTTCC	CGTACGC
Constant oligonucleotide	CO	P-GGAATCCCCC T GGGGGATTCC GCGTACG-OH (Aminated dT for immobilization is in bold)		

CO contained hydroxyl at 3′ end and phosphate at 5′ end, and the TOs had hydroxyl at both 3′ and 5′ ends.

3.1.2.2 Scheme of dsDNA Microarray Fabrication

The scheme of dsDNA microarray fabrication is illustrated in Figure 16.7. The main procedures were as followings. Firstly, the CO was denatured and reannealed in tube for forming hairpin-overhang structure. Secondly, the annealed CO was distributed into tubes containing variant denatured TOs, the mixtures were incubated at proper temperature for CO/TO hybridization. After hybridization, bimolecular hairpin oligonucleotides with a long overhang were formed, which, however, contained a nick in hairpin structure. Thirdly, the DNA ligase was added into CO/TO hybridization reaction for eliminating the nick and thus forming unimolecular hairpin oligonucleotides with a long overhang. Fourthly, the CO/TO unimolecular hairpin oligonucleotides were microspotted and immobilized on aldehyde-derivatized glass surface by the primary NH_2 group on the internal dT of CO. After the procedure, the partial-dsDNA microarrays were fabricated. At last, the 3′ end hydroxyls of immobilized unimolecular hairpin oligonucleotides were elongated by DNA polymerase on the template of 5′ end single-stranded overhangs. After the Klenow polymerization, the partial-dsDNA microarrays were converted into complete dsDNA microarrays which harbored the DNA-binding sites of sequence-specific DNA-binding proteins.

3.1.2.3 Verification of CO/TO Annealing and Ligation

To confirm the formation of unimolecular hairpin oligonucleotides by TO/CO annealing and ligating reactions, we synthesized a 5′-end FAM-labeled AP2

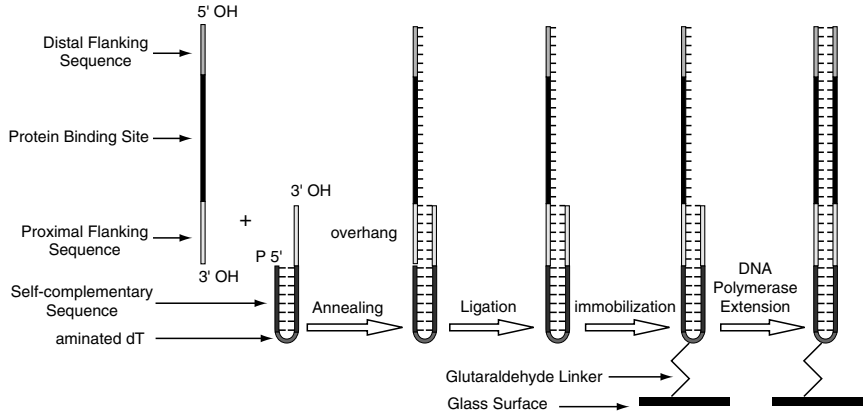

FIGURE 16.7. Scheme of dsDNA microarray fabrication with method 2.

TO and prepared three spotted DNA samples with it. The first was FAM-labeled AP2 TO annealed and ligated with CO, the second was FAM-labeled AP2 TO annealed but not ligated with CO, the third was FAM-labeled AP2 TO itself. The prepared three DNA samples were spotted on aldehyde-derivatized slides in triplet format. After immobilization, the slides were washed with $2 \times$ SSC/0.01% SDS and the fluorescence signals were collected with the standard FAM filter by laser scanning confocal microscope (Leica TCS SP) employing a 488 nm Ar ion laser. The results were displayed in Figure 16.8, which revealed that the first and second DNA samples presented fluorescence signals, while the third DNA sample did not. As without primary NH_2 group, the third DNA sample of FAM-labeled AP2 TO itself could not immobilize on glass slides and shed fluorescence signals, which confirmed the fluorescence signals displayed by the first and second DNA samples were CO-dependent. This implied that the FAM-labeled AP2 TOs in the first and second DNA samples annealed to COs. To further confirm the TO ligation with CO, the above signal-collected slides were denatured in 100 °C sterile ddH_2O for 10 min and then washed with $0.2 \times$ SSC/0.01% SDS. After washing, the slides were rescanned with previous laser channel. As expected, the fluorescence signals presented by the second DNA sample in previous scanning disappeared, while that from the first DNA sample still existed. This verified that the FAM-labeled AP2 TO in the first DNA sample was successfully ligated with CO into a unimolecular oligonucleotide. Therefore, the FAM linked at 5′ end of the unimolecular oligonucleotide could not be destroyed by denaturing treatment. However, the FAM-labeled AP2 TO in the second DNA sample broke away from immobilized CO in

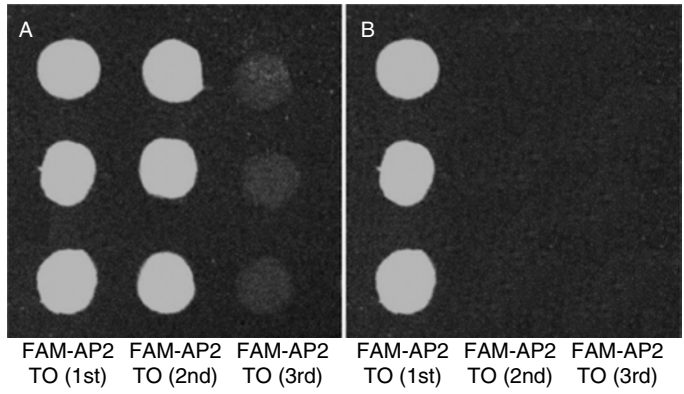

FIGURE 16.8. Fluorescence images of AP2 array before (A) and after (B) heat denaturation. FAM-AP2 TO (1st), FAM-AP2 TO (2nd) and FAM-AP2 TO (3rd) referred to FAM-labeled AP2 TO hybridized and ligated with CO, FAM-labeled AP2 TO hybridized but not ligated with CO, FAM-labeled AP2 TO itself respectively.

denature because it only annealed with CO to form the bimolecular oligonucleotides which could be melted by heat. In all, the unimolecular oligonucleotides for microspotting can be reliably fabricated by DNA ligase.

3.1.2.4 Validation of the Enzymatic Extension and Protein Binding to Microarray

To verify the Klenow polymerization, the Klenow extension reactions with Cy3-labeled dUTP instead of dTTP were done with the unimolecular oligonucleotides microarray fabricated by AP1, AP2, SP1, TFIID and NF-κB TOs listed in Table 16.1. The results were displayed in Figure 16.9A. It demonstrated that the fluorescence signals were seen over the entire arrays incubated with Klenow reaction containing Cy3-dUTP, while no signal appeared over the control arrays incubated with Klenow reaction without Cy3-dUTP (not shown). The Klenow-dependent presentation of fluorescence signals confirmed the occurrence of Klenow polymerization on immobilized short unimolecular hairpin oligonucleotides. We subsequently examined the accuracy of Klenow polymerization by sequence-specific restriction endonuclease digestion. The above signal-presented microarrays were incubated with HaeIII digestion reaction. The HaeIII-digested microarrays were rescanned and fluorescence signals were displayed in Figure 16.9B, which demonstrated the fluorescence intensities of AP2 spots greatly decreased. It agreed with the fact that only AP2 unimolecular dsDNA oligonucleotide harbored HaeIII digestion site (–GGCC-) and only two 5′

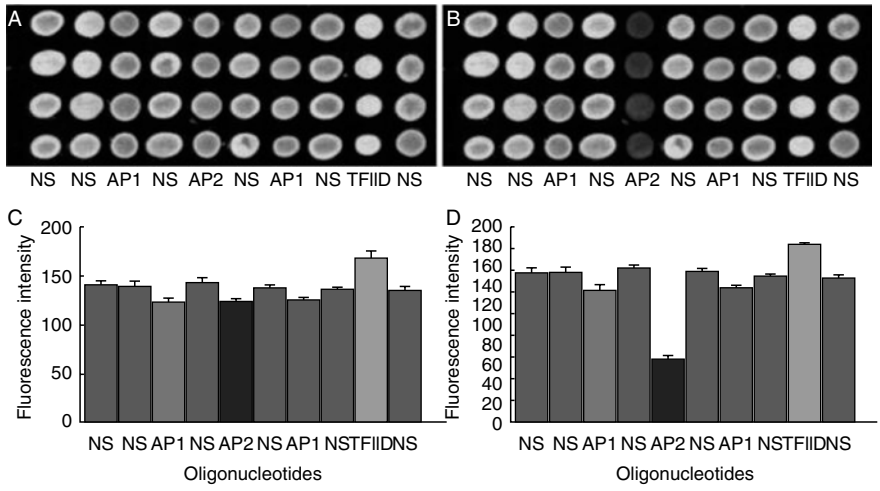

FIGURE 16.9. Fluorescence images and intensity plots of unimolecular dsDNA microarray fabricated by Klenow extension containing Cy3-labeled dUTP before (A and C) and after (B and D) HaeIII digestion in method 2.

end-anchored adenines in AP2 target oligonucleotide allowed Cy3-dUTP incorporation in Klenow polymerization. Therefore, we concluded that the Klenow extension could reach the distal terminals of immobilized oligonucleotides, and the high-fidelity enzymatically synthesized unimolecular dsDNA oligonucleotides on slides were accessible to sequence-specific restriction endonuclease.

The homogeneity of the dsDNA polymerization reactions on larger microarray and the accessibility of DNA-binding proteins to dsDNA microarray probes were demonstrated by the following 6×7 microarray fabrication with Cy3-labeled dUTP incorporation and Cy3-labeled NF-κB p50 binding to microarray fabricated with four label-free dNTP incorporation (Figure 16.10).

3.1.2.5 Specificity of NF-κB p50 Homodimer Binding to DNA Targets on dsDNA Microarray

As we aimed at fabricating unimolecular dsDNA microarray with general application value of study sequence-specific interactions between of DNA-binding proteins and dsDNA targets, we examined the sequence-specific accesiblity of transcription factor NF-κB to its target oligonucleotides immobilized on slides. We fabricated the unimolecular dsDNA microarrays with AP1, AP2, SP1, TFIID and NF-κB target oligonucleotides by Klenow reaction with unlabeled dNTPs. The fabricated microarrays were hybridized with Cy3-labeled NF-κB p50 homodimer and the scanned fluorescence signals were represented by Figure 16.11, which demonstrated that the NF-κB p50

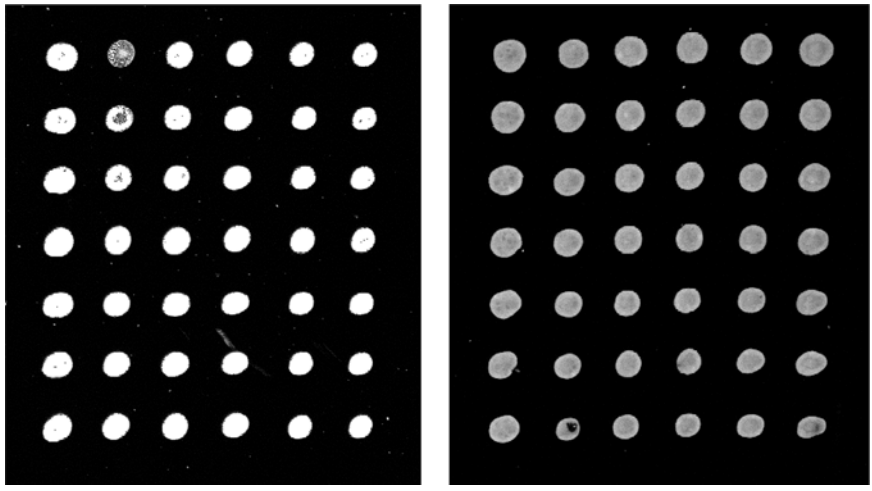

FIGURE 16.10. The homogeneous dsDNA microarray fabrication by Cy3-labeled dUTP DNA polymerase incorporation and the binding of Cy3-labeled NF-kB homodimer p50 to the dsDNA microarray fabricated with dNTP incorporation.

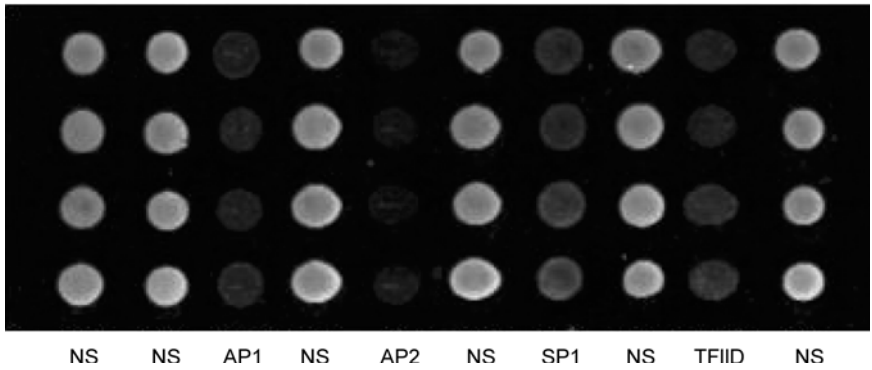

FIGURE 16.11. dsDNA microarray containing 9 different DNA-binding proteins targets which bound by Cy3-labeled NF-kB homodimer p50. The image demonstrated the sequence-specificity of interaction between arrayed dsDNA with protein.

homodimer specifically bound to its target oligonucleotides on slides. To further verify the sequence-specificity, we hybridized 6 similar unimolecular dsDNA microarrays anchoring 6×7 NF-κB TOs (NS in Table 16.2) with 6 variant binding reactions containing the same concentrations of Cy3-labeled NF-κB p50 homodimer but 6 different concentrations of cold free NF-κB dsDNA consensus oligonucleotides (Promega) sequencing identical to NS oligonucleotide. The results were displayed in Figure 16.5, which demonstrated that the fluorescence intensities decreased with the increase of cold free NF-κB dsDNA consensus oligonucleotides in binding reactions. It revealed that the binding of NF-κB to immobilized dsDNA targets could be restrained by specific competition. In all, the short unimolecular dsDNA oligonucleotides immobilized on slides could be specifically bound by DNA-binding protein as transcription factor.

3.1.2.6 Sensitivity of Detecting NF-κB p50 Homodimer with dsDNA Microarray

The capability of quantifying DNA-binding protein in detected samples by the unimolecular dsDNA microarray is very useful for the application of the dsDNA microarrays in detecting DNA-binding proteins. To determine the detecting sensitivity of target DNA-binding proteins with unimolecular dsDNA microarray, we hybridized 6 similar dsDNA microarrays anchoring 6×7 NF-κB TOs (NS in Table 16.2) with 6 binding reactions containing 6 different concentrations of Cy3-labeled NF-κB p50 homodimer. The results were displayed in Figure 16.12, which revealed that the signal intensities of microarrays coordinately decreased with the concentration of Cy3 labeled NF-κB in samples. The dsDNA microarray allowed detection of Cy3

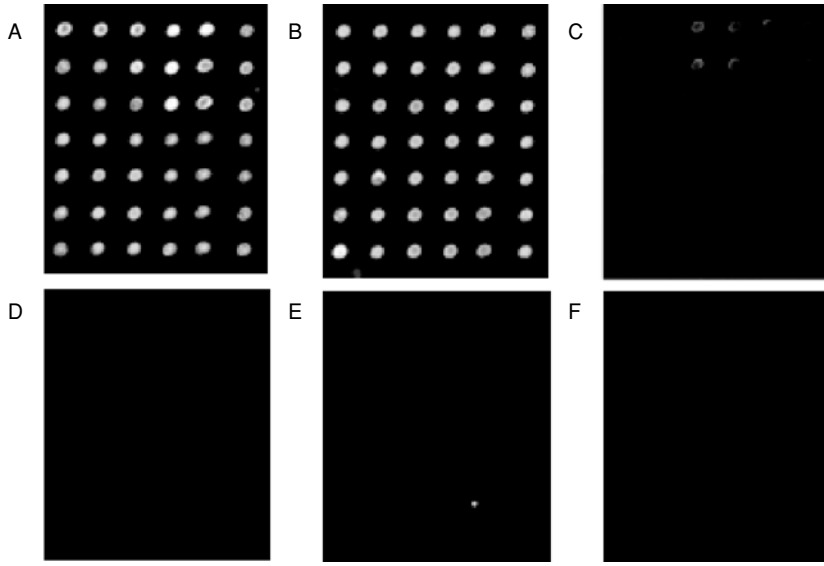

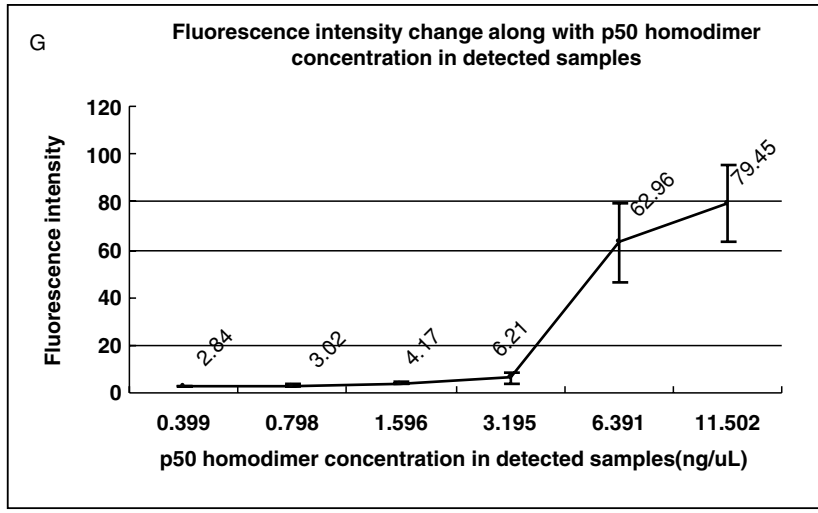

FIGURE 16.12. Fluorescence images and intensity plot of 6 dsDNA microarrays containing 6×7 NF-κB TOs hybridized with 6 variant binding reactions containing 6 different concentrations of Cy3-labeled NF-κB.

labeled NF-kB as few as 0.4ng/μl (0.8mol/ml) with very few protein sample (3μl enough for 6×7 spots array, 200μm spot diameter and 300μm spots interval).

3.2 dsDNA Microarray Application: Evaluating the Binding Affinities of NF-κB p50 Homodimer to Wild-Type and Single-Nucleotide Mutations Ig-κB Sites (Method 2)

To high-throughput quantify the binding affinities of NF-κB to variant DNA targets, we fabricated the unimolecular dsDNA microarrays containing the wild-type and all possible single-nucleotide mutant I*g*-κB sites and examined the binding affinities of NF-κB (p50 homodimer) to all targets. We hope to define the importance of each nucleotide consisted of 10-base I*g*-κB for NF-κB (p50 homodimer) binding with I*g*-κB which naturally exists in immunoglobulin light chain κ gene and HIV-LTR. We took the 5′-GGGAC-3′ and 5′-TTCC-3′ as two subsites respectively bound by two p50 monomers and numbered the nucleotides from 5′ to 3′ end as showed in Table 16.3. The microarrays were hybridized with Cy3-labeled NF-κB p50 homodimer.

The results were displayed in Figure 16.13. It was clearly demonstrated that the binding affinities of p50 homodimer to 30 single-nucleotide mutant I*g*-κBs were almost all lower than that of p50 homodimer with wild-type I*g*-κB site. However, the binding affinities of p50 homodimer to 30 single-nucleotide mutated I*g*-κBs were greatly different from each other.

TABLE 16.3. DNA sequences of wild-type NF-κB binding sites

No.	DNA sequence (5′→3′)	No.	DNA sequence (5′ →3′)
1CIg-κB	AGTTGAGCGGACTTTCCCAGGC	6G Ig-κB	AGTTGAGGGGACGTTCCCAGGC
1A Ig-κB	AGTTGAGAGGACTTTCCCAGGC	6C Ig-κB	AGTTGAGGGGACCTTCCCAGGC
1T Ig-κB	AGTTGAGTGGACTTTCCCAGGC	6A Ig-κB	AGTTGAGGGGACATTCCCAGGC
2C Ig-κB	AGTTGAGGCGACTTTCCCAGGC	7G Ig-κB	AGTTGAGGGGACTGTCCCAGGC
2A Ig-κB	AGTTGAGGAGACTTTCCCAGGC	7C Ig-κB	AGTTGAGGGGACTCTCCCAGGC
2T Ig-κB	AGTTGAGGTGACTTTCCCAGGC	7A Ig-κB	AGTTGAGGGGACTATCCCAGGC
3C Ig-κB	AGTTGAGGGCACTTTCCCAGGC	8G Ig-κB	AGTTGAGGGGACTTGCCCAGGC
3A Ig-κB	AGTTGAGGGAACTTTCCCAGGC	8C Ig-κB	AGTTGAGGGGACTTCCCCAGGC
3T Ig-κB	AGTTGAGGGTACTTTCCCAGGC	8A Ig-κB	AGTTGAGGGGACTTACCCAGGC
4T Ig-κB	AGTTGAGGGGTCTTTCCCAGGC	9G Ig-κB	AGTTGAGGGGACTTTGCCAGGC
4G Ig-κB	AGTTGAGGGGGCTTTCCCAGGC	9A Ig-κB	AGTTGAGGGGACTTTACCAGGC
4C Ig-κB	AGTTGAGGGGCCTTTCCCAGGC	9T Ig-κB	AGTTGAGGGGACTTTTCCAGGC
5G Ig-κB	AGTTGAGGGGAGTTTCCCAGGC	10G Ig-κB	AGTTGAGGGGACTTTCGCAGGC
5A Ig-κB	AGTTGAGGGGAATTTCCCAGGC	10A Ig-κB	AGTTGAGGGGACTTTCACAGGC
5T Ig-κB	AGTTGAGGGGATTTTCCCAGGC	10T Ig-κB	AGTTGAGGGGACTTTCTCAGGC
Wild-type Ig-κB	AGTTGAGGGGACTTTCCCAGGC	Base No.	**GGGACTTTCC 12345678910**
Constant	P-GGAATCCCCC *T* GGGGGATTCC GCGTACG-OH (*T*: Aminated dT)		
note	Both 5′ and 3′ ends of target oligonucleotides are hydroxyl.		

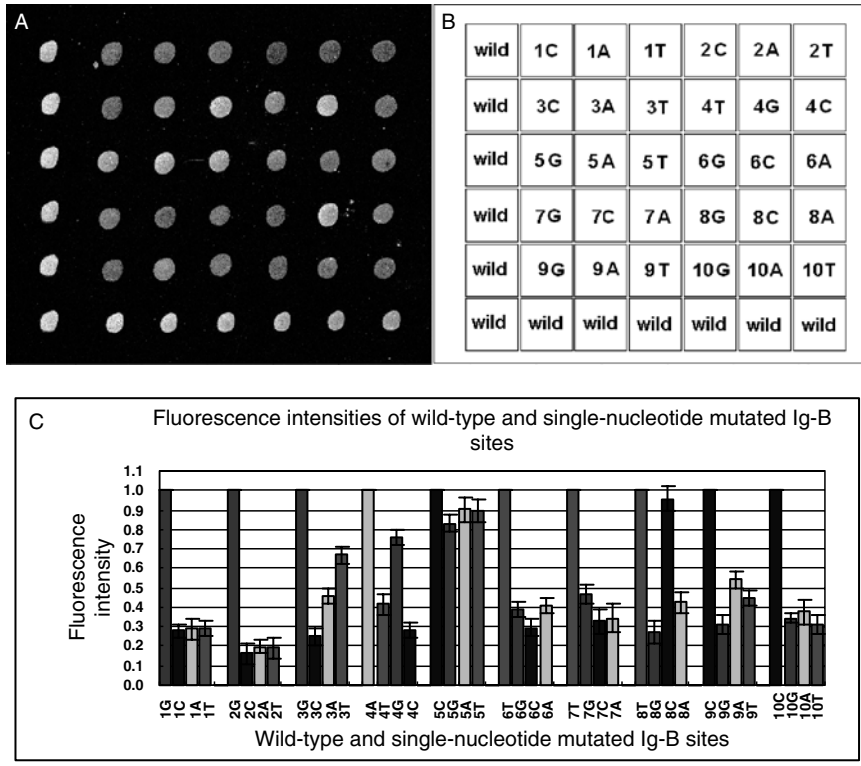

FIGURE 16.13. Fluorescence image and intensity plot of unimolecular dsDNA microarray. (A) One fluorescence image of dsDNA microarray with wild-type and single-nucleotide mutated Ig-κB sites, which was hybridized with Cy3 labeled NF-κB p50 homodimer. (B) DNA targets positions on dsDNA microarray. (C) Plot of statistical fluorescence intensities of 10 dsDNA microarrays.

In 5′-GGGAC-3′ subsite, the guanosines at positions 1 and 2 were most important for high-affinity binding of NF-κB (p50 homodimer) to Ig-κB, as any other three nucleotides replacements of those two guanosines resulted in similar great affinity loses. However, there was still a little difference between the two guanosines. The mutations of guanosine at position 2 presented more affinity loses than that of guanosine at position 1. The guanosine at position 3 is less important for p50p50 /Ig-κB interaction than that at position 2. Its replacements with different nucleotides resulted in distinct binding affinities. The binding affinities of p50 homodimer to the three mutated Ig-κBs became lower as the order of substitution of the 3G with T, A and C. The exchange of the guanosine into cytosine at position 3 resulted in the largest decrease of binding affinity, while the guanosine at position 3 could tolerate A or T substitution. As adenine at position 4 was replaced with G, T

and C respectively, the binding affinity loses were different from each other. It was obvious that the nucleotide at position 4 preferred purines other than pyrimidines. All single-nucleotide mutations of cytosine at the position 5 presented the little binding affinity loses. Namely, no matter the cytosine at the position 5 were changed into any other three nucleotides, only a little decrease of the binding affinity happened compared to wild-type I*g*-κB site. The adenine and cytosine at position 5 were more beneficial for protecting binding affinity of p50 homodimer to I*g*-κB than guanosine.

Compared with the mutation in 5′-GGGAC-3′ subsite, most of the single-nucleotide mutations at 5′-TTCC-3′subsite resulted in greater affinity lose in NF-κB (p50 homodimer) binding to I*g*-κB. However, the single-nucleotide exchange of thymine into cytosine at position 8 had little effect on high-affinity binding of p50 homodimer to mutant I*g*-κB. Moreover, this mutation produced obvious higher binding affinities than wild-type I*g*-κB in several experiments. Except the marked affinitiy holding in cytosine replacement at position 8, the exchange of cytosine into adenine at position 9 was more helpful for keeping binding affinity of p50 homodimer to I*g*-κB than other single-nucleotide mutations. Any mutations of cytosine at position 10 could not avoid significant affinity decrease in p50 homodimer binding with I*g*-κB. It was noteworthy that the mutations at the axle thymine resulted in significant binding affinity loses.

The results from the unimolecular dsDNA microarray could be steadily repeated on the different microarrays (Fig. 16.14).

4. Discussion

The Church's lab saw the great potentials of dsDNA microarray for studying sequence-specific DNA/protein interaction(34), and fabricated dsDNA microarray for exploring the DNA-binding specificities of zinc fingers with arrayed DNA targets (38, 39). Their creative works verified the feasibility and high effectiveness of dsDNA microarray in studying sequence-specific DNA/protein interaction. Nevertheless, their dsDNA microarray fabrication replied on the Affymetrix proprietary technology of photo-addressable oligonucleotide synthesis which is unaffordable for general laboratories until now. In this paper, we presented two novel methods for fabricating unimolecular dsDNA microarray and verified its reliability. These methods have several significant advantages. Firstly, considering the expensive amino-labeling of oligonucleotides which cost was almost identical to target oligonucleotide synthesis (about 25 base pairs), the free constant oligonucleotide with amino modifier C6 dT was adopted to avoid repeatedly synthesizing long constant oligonucleotide with C6dT on each target oligonucleotides. This strategy can dramatically decrease the cost of unimolecular dsDNA microarray manufacture. Secondly, with free constant C6dT oligonucleotide, we only need to chemically synthesize target oligonucleotides for fabricating unimolecular dsDNA

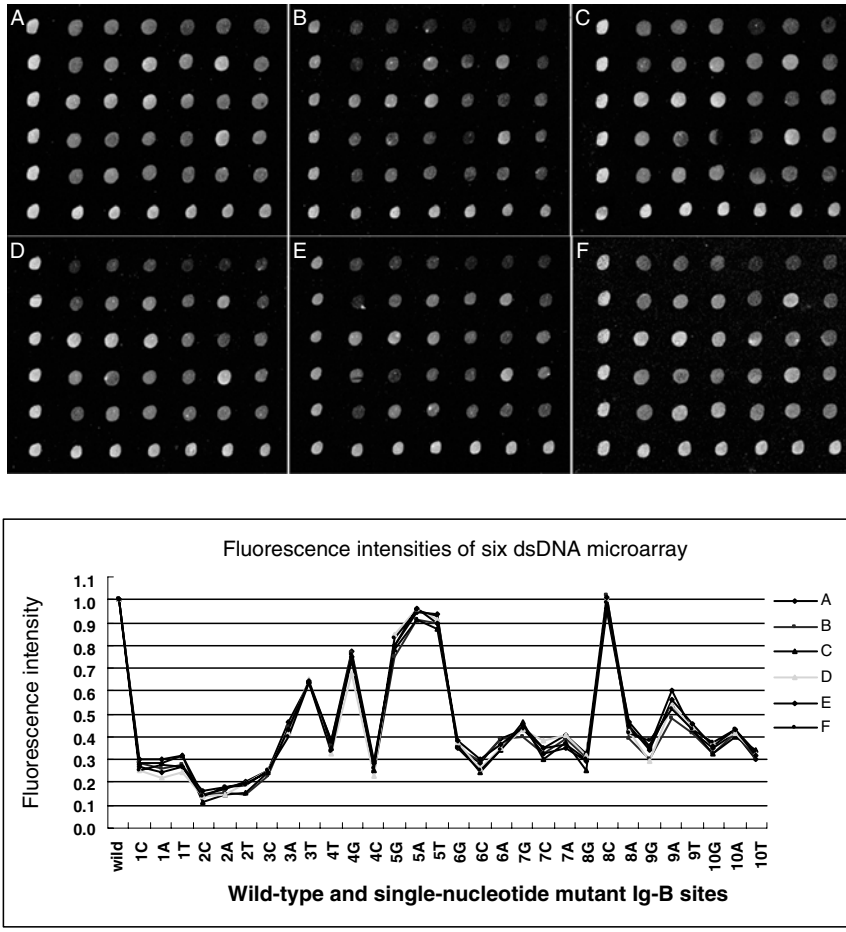

FIGURE 16.14. Fluorescence images and intensity plot of dsDNA microarrays on six different slides. (A-F) Fluorescence image of six dsDNA microarrays which were hybridized with Cy3 labeled p50 homodimer. (G) Fluorescence intensities plot of six dsDNA microarrays (A-F).

microarray. We testified that as short as 23bp (AP2) and 24bp (NF-κB) oligonucleotides harboring protein-binding sites were long enough for proteins binding interaction. To synthesize so short single-stranded oligonucleotides also greatly lowers the cost of unimolecular dsDNA microarray manufacture. It avoids synthesizing long self-complementary single-stranded oligonucleotides for fabricating dsDNA oligonucleotides by annealing (US patent 5556752). Thirdly, as the "second" complementary strands of oligonucleotides were enzymatically synthesized by DNA polymerase, it also greatly lowers the cost of unimolecular dsDNA microarray manufacture. Fourthly, as the exact

complements of immobilized target oligonucleotides were synthesized by high-affinity Klenow DNA polymerase I, this method is competent for fabricating dsDNA microarray containing generic or homogenous dsDNA oligonucleotides with similar sequences as single nucleotide polymorphism (SNP). It overcomes the impossibility of fabricating generic or homogenous dsDNA, especially SNP dsDNA microarrays by hybridization (35, 36). This is very important for dsDNA microarray applications to studying sequence-specific DNA/protein interactions. Fifthly, the enzymatically synthesized ultimate dsDNA oligonucleotides immobilized on glass were unimolecular nucleic acids, which can hold their function by reanneating after heat denature. Therefore, the unimolecular dsDNA microarray can be used for many times by removing bound proteins with stringent washing or heat denaturing. This far differs from bimolecular-dsDNA microarray (34-39). Finally, this method of unimolecular dsDNA microarray fabrication accommodates with commercially available microarray spotting robots, it is reachable for extensive application.

For high-throughput investigation of binding affinities of a larger number of DNA targets with NF-κB transcription factors, we fabricated the special unimolecualar dsDNA microarray with a novel scheme to examine the binding affinities of NF-κB p50 homodimer with the wild-type and single-nucleotide mutant I*g*-κB sites. We thereby assessed the importance of each nucleotide of I*g*-κB to p50-p50/I*g*-κB binding interaction by the highly-paralleled microarray pattern. Our studies revealed that each nucleotide of I*g*-κB site contributes differently to p50-p50/I*g*-κB binding interaction. These findings were useful for not only redefining the role of nucleotides at different positions of I*g*-κB site, but also predicting the potential NF-κB-binding targets. The data from unimolecualar dsDNA microarray could be used to pinpoint the base-amino acid contacts in DNA/NF-κB interaction. The crossvalidations of our dsDNA microarray data with that from crystallography, EMSA and statistic model demonstrated that the unimolecular dsDNA microarray provided a valuable general method for exploring the binding affinities of a larger number of DNA targets with DNA-binding proteins or DNA-binding drugs.

Our experiments revealed that the sequence-specific DNA-binding proteins as restriction endonuclease and transcription factor in detected samples could sensitively and specifically bind with dsDNA targets immobilized on microarray. This demonstrates that the unimolecular dsDNA microarray fabricated with our method provides a novel stable high-throughput technique for investigation of DNA/protein interactions. The unimolecular dsDNA microarray should be potentially used to studies including (1) screening sequence-specific DNA-binding proteins, (2) predicting new DNA-binding sites of transcription factors in genome, (3) assessing importance of nucleotides in DNA-binding sites for DNA/protein interactions, (4) monitoring the expression of drug-induced DNA-binding proteins, and (5) screening sequence-specific DNA-binding drugs.

Acknowledgement. This work is supported by the National Natural Science Foundation of China (60201005) and the National Science Fund for Distinguished Young Scholars (60121101).

References

1. Pabo, C.O. and Sauer, R.T. (1992) *Annu. Rev. Biochem*., 61, 1053–1095.
2. Craig, N.L. (1988) *Annu. Rev. Genet*., 22, 77–105.
3. Pingoud, A. and Jeltsch, A. (1997) *Eur. J. Biochem*., 246, 1–22.
4. Margulies, C. and Kaguni, J.M. (1996) *J. Biol. Chem*., 271, 17035–17040.
5. Brazil, M. (2002) *Nature* 1, 9.
6. Chaires, J.B. (1998) *Current Opinion in structural biology* 8, 314–320
7. Woodbury, C.P. & Hippel, P. H.V. (1983) *Biochem*. 22, 4730–4737.
8. Jansen, C., Gronenborn, A.M. & Clore, G.M. (1987) *Biochem. J.*, 246, 227–232.
9. Ruscher, K., Reuter, M., Kupper, D., Trendelenburg, G., Dirnagl, U., Meisel, A. (2000) *J. Biotech*., 78, 163–170.
10. Bowen, B., Steinberg, J., Laemmli, U.K. and Weintraub, H. (1980) *Nucleic Acids Res*., 8, 1–20.
11. Miskimins, W.K., Roberts, M.P., McClelland, A. and Ruddle, F.H. (1985) *Proc. Natl. Acad. Sci. USA*, 82, 6741–6744.
12. Choo, Y. and Klug, A. (1993) *Nucleic Acids Res*., 21, 3341–3346.
13. Hanes, S.D. and Brent, R. (1991) *Sci*ence 251, 426–430.
14. V. Olando. (2000) *Trands Biochem. Sci*., 25, 99–104.
15. Rebar, E.J. and Pabo, C. O. (1994) *Sci*., 263, 671–673.
16. Choo, Y. and Klug, A. (1993) *Proc. Natl. Acad. Sci. USA* 91, 11168–11172.
17. Oliphant, A., Brendl, C. and Struhl, K. (1989) *Mol. Cell Biol*. 9, 2944–2949.
18. Escolano, A.L.G.R., Medina, F., Racaniello, V. R., and Angel, R. M. D. (1997) *Virol*. 227, 505–508.
19. Bilanges, B., Varrault, A., Basyuk, E., Rodriguez, C., Mazumdar, A., Pantaloni, C., Bockaert, J., Theillet, C., Spengler, D., Journot, L. (1999) *Oncogene* 18, 3979–3988,.
20. Müller, C. W., Rey, F. A., Sodeoka, M., Verdine, G. L. & Harrison, S. C. (1995) *Nature* 373, 311–317.
21. Ghosh, G., vanDuyne, G., Ghosh, S. & Sigler, P.B. (1995) *Nature* 373, 303–310.
22. Dougherty, G. & Pigram, W. J. (1982) *CRC Crit. Rev. Biochem*. 12, 103–132.
23. Zimmer, C. & Luck, G. (1992) In Hurley, L. H. (ed.), Advances in DNA Sequence Specific Agents. JAI Press Inc., London, UK, Vol. 1, pp. 51–88.
24. Searle,M.S. (1993) *Prog. NMR Spectrosc*. 25, 403–480.
25. Chaires, J.B. (1992) In Hurley, L. H. (ed.), Advances in DNA Sequence Specific Agents. JAI Press Inc., London, UK, Vol. 1, pp. 3–23.
26. Imad I. Hamdan, Graham G. Skellern and Roger D. Waigh. (1998) *Nucleic Acids Res*., 26, 3053–3058.
27. Coury, J. E., McFail-lsom, L., Williams, L.D., & Bottomley, L. A. (1996) *Proc. Natl. Acad. Sci. USA*, 93, 12283–12286.
28. Coury, J. E., Anderson, J. R., McFail-lsom, L., Williams, L. D. & Bottomley, L. A. (1997) *J. Am. Chem. Soc*. 119, 3792–3796.
29. Joseph E. Coury, Lori Mcfail-Isom, Loren Dean Williams, and Lawrence A. Bottomley. (1996) *Proc. Natl. Acad. Sci. USA* 93, 12283–12286.

30. Torunn Berge, Nigel S. Jenkins, Richard B. Hopkirk, Michael J. Waring, J. Michael Edwardson, Robert M. Henderson. (2002) Accepted for publication in 'Nucleic Acids Research', 15 May, 2002.
31. Gambari R, Feriotto G, Rutigliano C, Bianchi N, Mischiati C (2000) *J. Pharmacol. Exp. Ther*. 294, 370–377.
32. Passadore M, Feriotto G, Bianchi N, Aguiari G, Mischiati C, Piva R, Gambari R. (1994) *J. Biochem. Biophys. Methods* 29, 307–19.
33. M Broggini, M Ponti, S Ottolenghi, M D'Incalci, N Mongelli and R Mantovani. *Nucleic Acids Res*. 17, 1051–1059.
34. Bulyk, M. L., Gentalen, E., Lockhart, D. J. & Church, G. M. (1999) *Nat. Biotechnol*., 17, 573–577.
35. Drobyshev, A.L., Zasedatelev, A.S., Yershov, G.M. & Mirzabekov, A. D. (1999) *Nucleic Acids Res*., 27, 4100–4105.
36. Krylov, A. S., Zasedateleva, O. A., Prokopenko, D. V., Rouviere-Yaniv, J. & Mirzabekov, A. D. (2001) *Nucleic Acids Res*., 29, 2654–2660.
37. Nordhoff, E., Krogsdam, A.M., Jorgensen, H.F., Kallipolitis, B.H., Clark, B.F.C., Roepstorff, P. & Kristiansen, K. (1999) *Nat. Biotechnol*., 17, 884–888.
38. Bulyk, M. L., Huang X, Choo Y. & Church, G. M. (2001) *Proc. Natl. Acad. Sci. USA* 98, 7158–7163.
39. Bulyk, M. L., Johnson, P. L. F. & Church, G. M. (2002) *Nucleic Acids Res*., 30, 1255–1261.
40. Kadonaga, J.T. & Tjian, R. (1986) *Proc. Natl. Acad. Sci. USA* 83, 5889–5893.
41. Kadonaga, J.T. (1991) *Methods Enzymol*. 208, 10–23.
42. Lochart, D.J., Vetter, D. & Diggelmann, M. US patent # 5556752, issue date 9/17/96
43. Braun, E., Eichen, Y., Sivan, U. & Ben-Yoseph, G. *Nature* 391, 775–778 (1998).
44. McGall, G.H., Barone, A.D., Diggelmann, M., Fodor, S.P.A., Gentelen, E. & Ngo. N. (1997) *J. Am. Chem. Soc*. 119, 5081–5090.
45. Southern, E.M. et al. (1999) *Nat. Genet*. (Suppl.) 21, 5–9.
46. Carlson, R. & Brent, R. (1999) *Nat. Biotech*. 17, 536–537.
47. Kwiatkowski, M., Fredriksson, S., Isaksson, A., Nilsson, M. & Landegren, U. (1999) *Nucleic Acids Res*. 27, 4710–4714.
48. Craig, N.L. (1988) *Annu. Rev. Genet*., 22, 77–105.
49. Pingoud, A. and Jeltsch, A. (1997) *Eur. J. Biochem*., 246, 1–22.
50. Margulies, C. & Kaguni, J.M. (1996) *J. Biol. Chem*., 271, 17035–17040.
51. Jansen, C., Gronenborn, A.M. & Clore, G.M. (1987) *Biochem. J*., 246, 227–232.
52. Bowen, B., Steinberg, J., Laemmli, U.K. & Weintraub, H. (1980) *Nucleic Acids Res*. 8, 1–20.
53. Hanes, S.D. & Brent, R. (1991) *Sci*., 251, 426–430.
54. Schena, M., Shalon, D., Davis, R.W. & Brown, P.O. (1995) *Sci*., 270, 467–470.
55. DeRisi, J. L., Iyer, V. R. & Brown, P. O. *Science* 278, 680–686 (1997).